nature nanotechnology

SUPPLEMENTARY INFORMATION

DOI: 10.1038/NNANO.2013.55

A nanoscale combing technique for large-scale assembly of highly-aligned nanowires

Jun Yao, Hao Yan and Charles M. Lieber

This file includes:

Nanowire density analysis. The density of nanowire devices possible can be evaluated as follows. Specifically, the data shown in Fig. 2a provide density statistics that would yield a trimmed nanowire length of 4 μm, although we also point out that this length could be increased (and corresponding fraction of combing to anchoring area increased) by using longer nanowires on the growth substrate. Ignoring this latter point and using the data presented in Fig. 2a, we can examine an alternating patterning feature of 10 μm anchoring length, 10 μm combing length and 4 μm trimmed nanowire length: the measured density then yields 20% nanowire coverage and device density of $7 \times 10^6/cm^2$. We consider this a cautious estimate because it should be possible to reduce the combing length to close to the trimmed nanowire length (or increase the trimmed nanowire length for the large combing region) with the trimming process. For example, using an alternating patterning feature of 10 μm anchoring length, 5 μm combing length and a resultant 4 μm trimmed nanowire length would yield 27% nanowire coverage and a device density of 1×10^7 cm^{-2}. Note that crossbar architectures are an alternative and very attractive direction being pursued innanoelectronics[1]. If a crossbar type of architecture (and crossbar pitch of ref. 1) is used for the nanowire coverages/densities noted above, the FET density (i.e., a two-dimensional array) would be 7×10^7 cm^{-2} to 1×10^8 cm^{-2} , close to that in more traditional functional circuits[2].

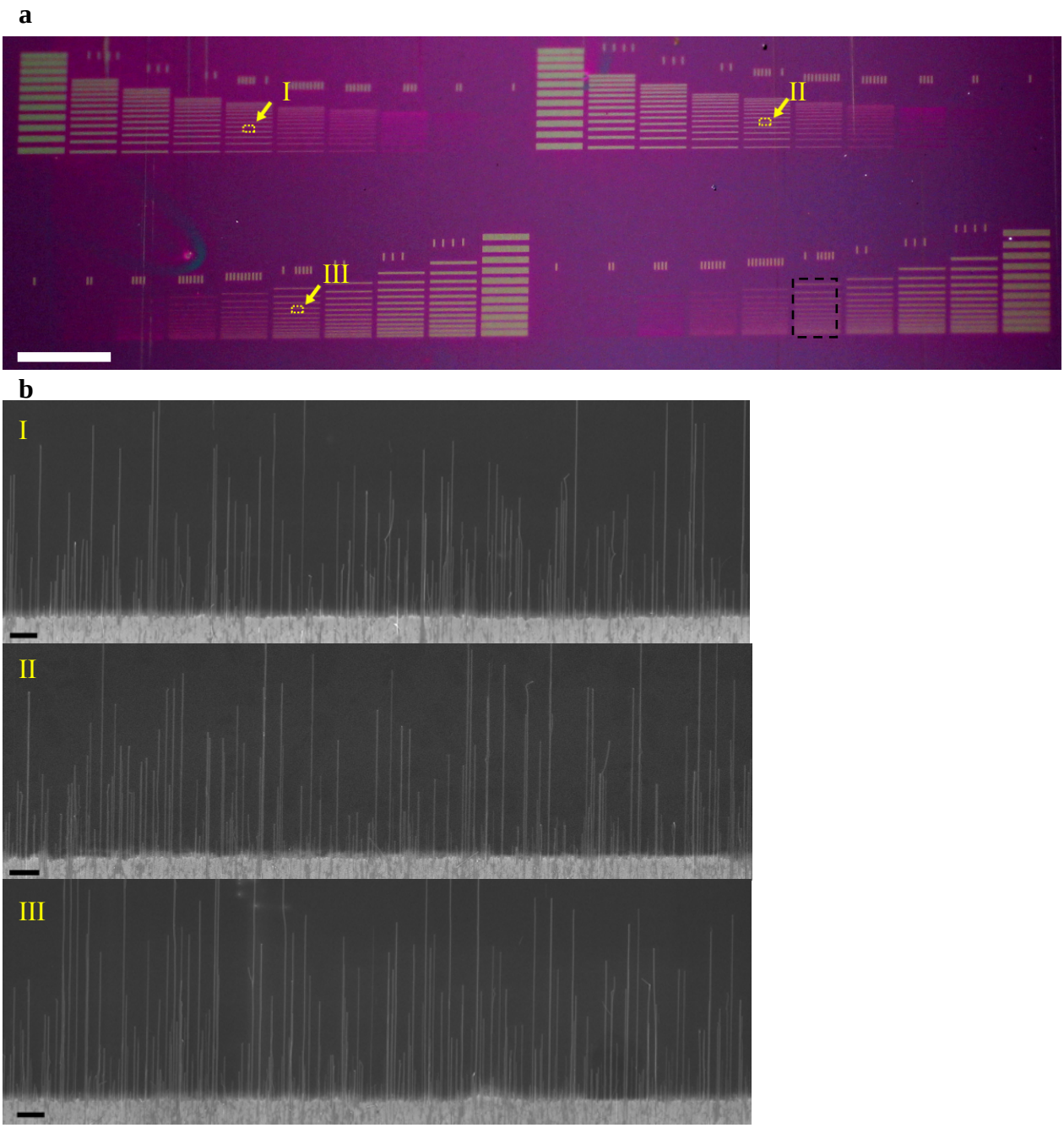

Figure S1 | Large area nanocombing. **a,** Optical micrograph of nanocombed nanowires over an ca. 3 mm × 11 mm area of a substrate chip. The bright regions visible in the image correspond to the anchoring regions. The image shows four blocks with each block containing ten columns of anchoring windows (bright stripes in the image) having anchoring lengths of 1, 2, 4, 7, 10, 15, 20, 30, 40, and 80 μm. The area enclosed by dashed black box in lower right quadrant indicates the region shown in Fig. 1b in the main paper. Scale bar, 1 mm. **b,** Representative SEM images of the nanocombed nanowires from the three blocks quadrants not shown in Fig. 1; each panel corresponding to the region indicated by dashed yellow box and number in **a**. Scale bars, 2 μm.

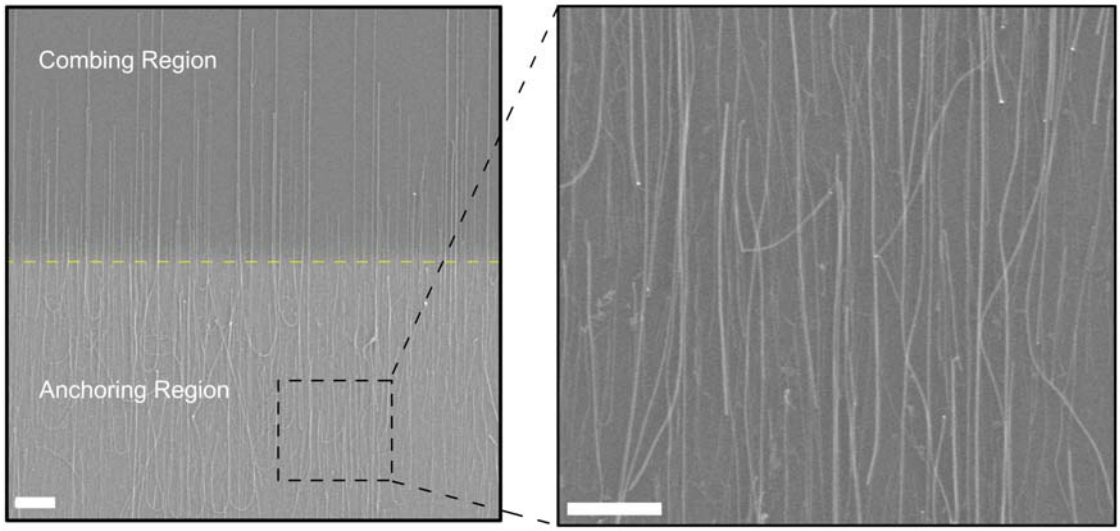

Figure S2 | Nanowire alignment comparison between combing and anchoring regions. The sample is the same as in Fig. 1 in the main text. (Left panel) SEM image of combed nanowires, where the image area includes both the anchoring region (functionalized SiO_2 surface) and combing region (resist surface). The dashed yellow line highlights the boundary between the two regions. Scale bar, 2 μm. (Right panel) An enlarged SEM image of the nanowires in the anchoring region indicated by the dashed box in the left panel. Scale bar, 1 μm.

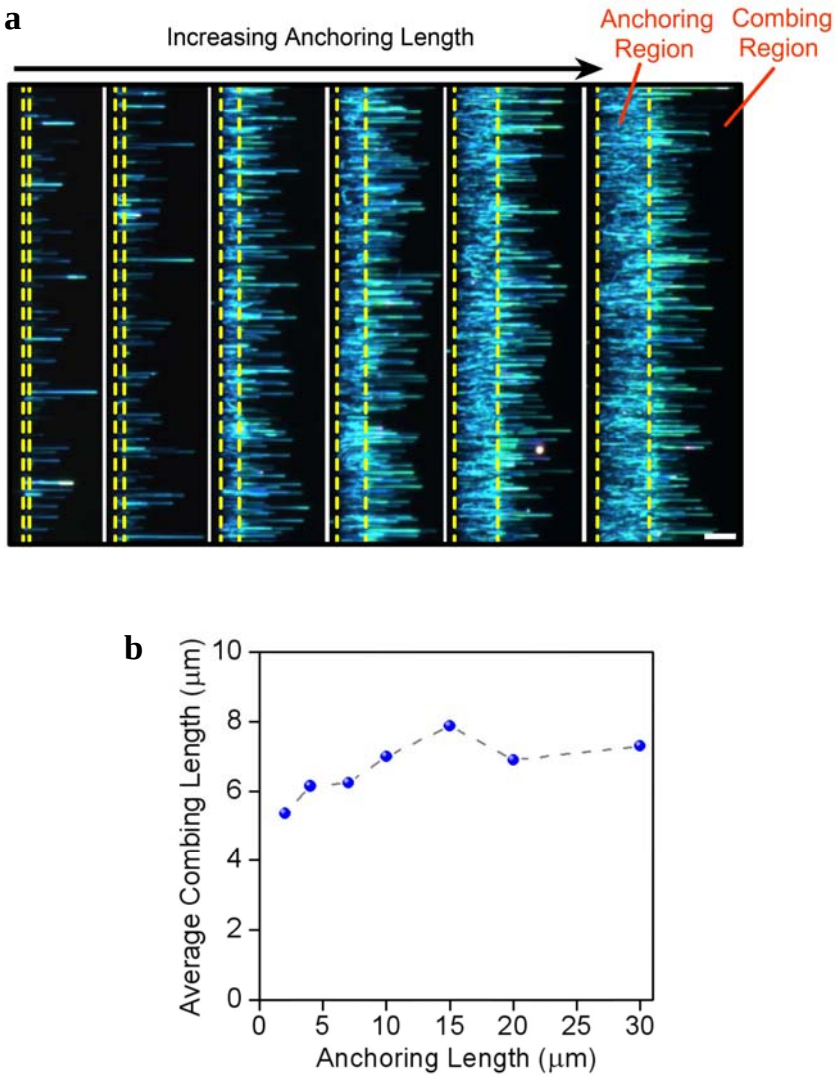

Figure S3 | Statistics of nanowire length. **a,** Dark-field optical microscopy images of the combed nanowires for anchoring lengths 2, 4, 7, 10, 15 and 20 μm, left to right, respectively. The resist layer is present in the combing regions and the sample is the same as in Fig. 1 in the main text. Scale bar in right most panel, 10 μm, is same for all images. **b,** Average combing length with respective to different anchoring lengths. At the saturated nanowire combing density (anchoring length > 10 μm), the average combing length is ~ 7.3 μm. The average growth length of ~ 30 μm yielded an average transferred length (including the anchoring part) ~ 15 μm. This yields a ratio of ~ 1:1 between the average anchoring length and combing length.

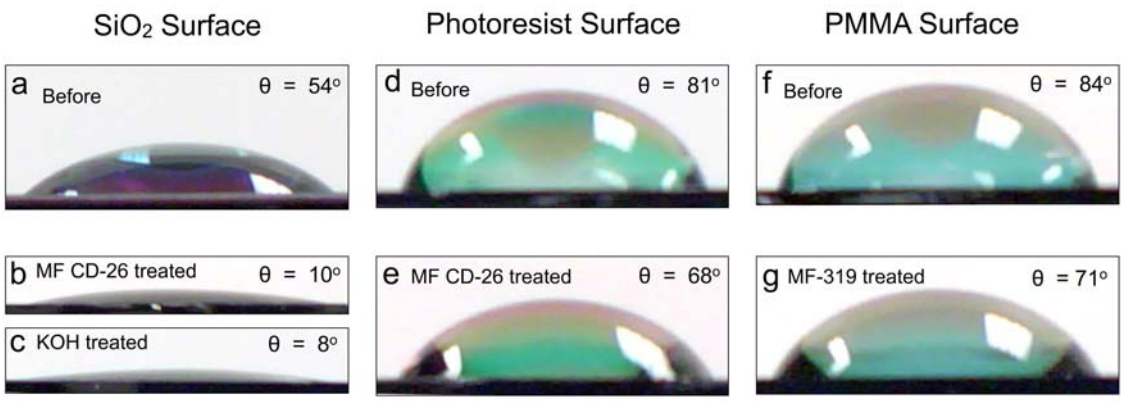

Figure S4 | Contact angle measurements. Contact angles on **a,** SiO_2 surface (without any treatment); **b,** SiO_2 surface treated with 50 s MF CD-26; **c,** SiO_2 surface treated with 50 s KOH solution (1.5 wt%); **d,** photoresist (S1805) surface (without any treatment); **e,** photoresist surface treated with 50 s MF CD-26; **f,** PMMA surface (without any treatment); **g,** PMMA surface treated with 50 s MF-319. The functionalized surfaces were then cleaned in deionized (DI) water (e.g., ~ 10 s). Here the procedures are the same as those adopted in nanocombing on photoresist or PMMA surfaces described in the main text.

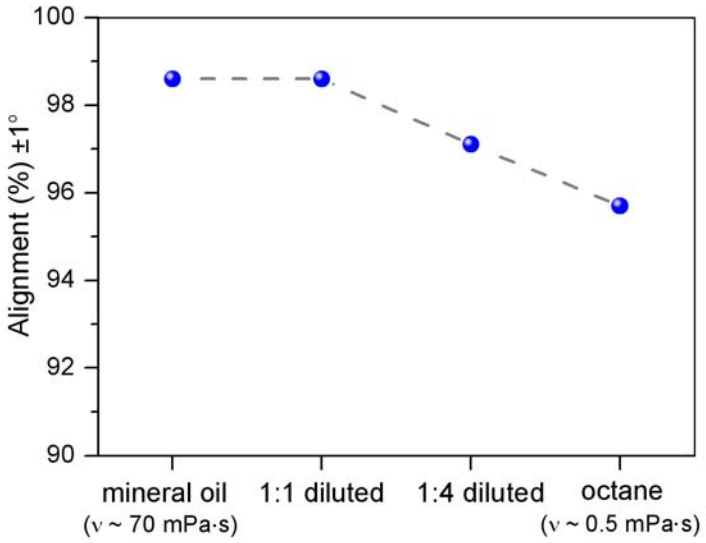

Figure S5 | Nanowire-alignment dependence on the viscosity of the lubricants. The mineral oil (heavy) used as a lubricant in the main text has a viscosity (ν) ~ 70 mPa·s. Different reduced viscosities were obtained by diluting the heavy oil in octane (ν ~ 0.5 mPa·s). New experiment also showed that very few nanowires were attached to the substrate using isopropyl alcohol (IPA) as the transfer liquid, where nanowires formed a stable suspension in IPA but not in mineral oil. These data, which were acquired with constant normal force during nanocombing, demonstrate that the high viscosity of the oil is not critical for nanocombing but rather the hydrophobic character, which is consistent with the model. In addition, these results as well as the original pressure-dependent measurements (inset, Fig. 2b) suggest that the amount of oil (sandwiched between the transfer and growth substrates) is not a major factor.

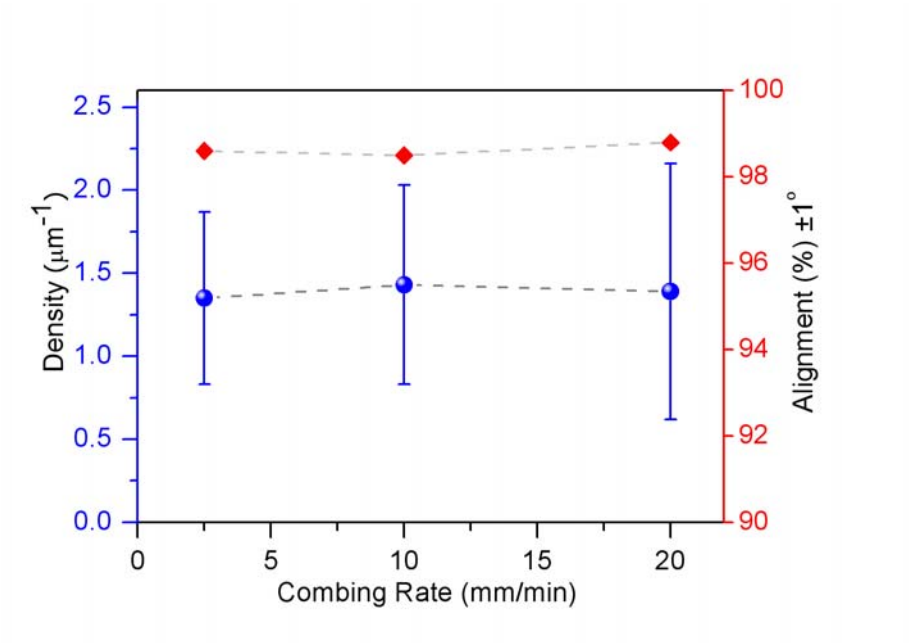

Figure S6 | Nanowire density and alignment dependence on the combing rate. The alignment criteria is defined the same as in the main manuscript, *i.e*. within ±1º of the combing direction. These data show that the density and alignment ratio are ca. independent of the combing speed within the tested range above, and thus suggest that following the attachment in the anchoring region the minimum necessary alignment force is lower than minimum shear value accessed (consistent with a weak nanowire/combing region interaction). The combing conditions were the same as adopted in Fig. 1 of the main text. The data are based on the anchoring length of 15 μm.

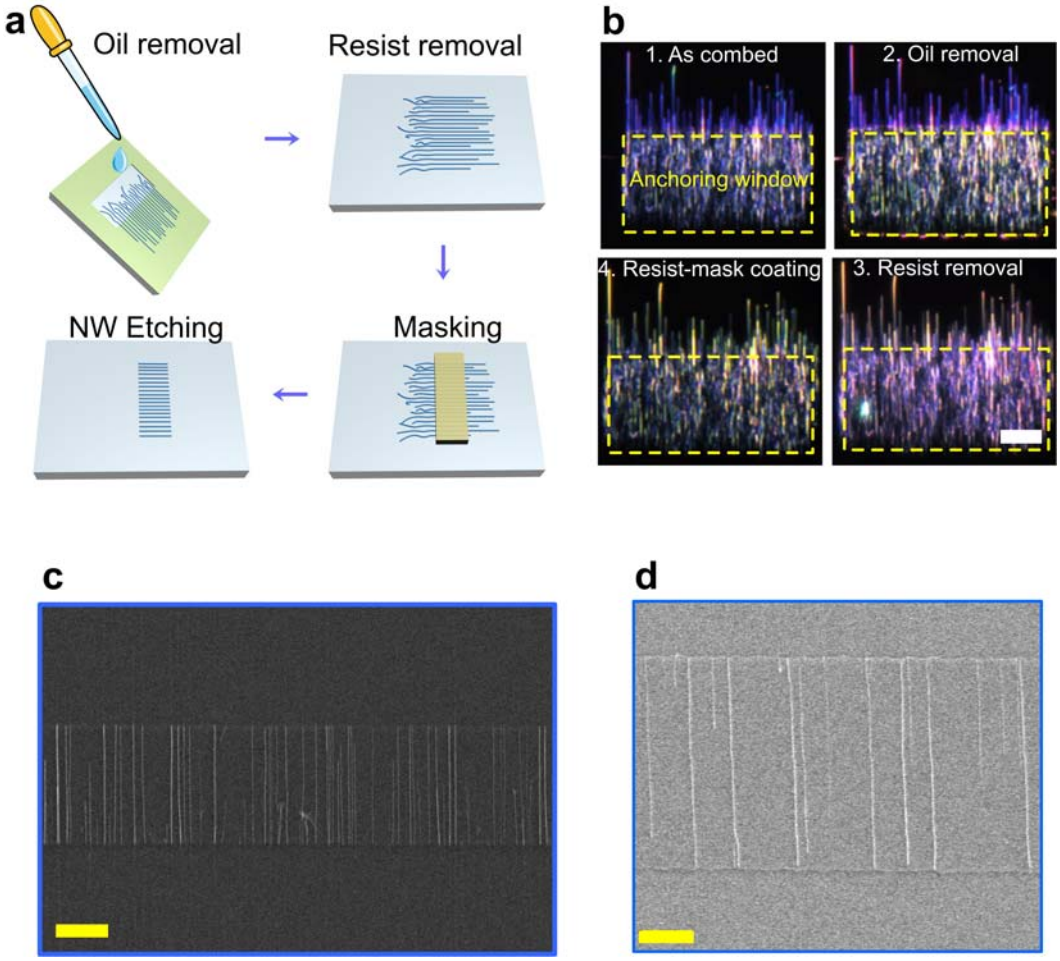

Figure S7 | Nanowire cleaning and nanowire trimming processes. **a**, Schematics of the cleaning and trimming processes. The oil transfer lubricant was removed gently by flowing drops of octane over the substrate followed by gentle drying with nitrogen. The underlying resist layer was removed by ultraviolet (UV)-ozone treatment (120 ºC, 15 min). UV-ozone was used to the removal S1805 and PMMA. For trimming, a masking layer (MMA + PMMA 950-C2) is spin-coated, patterned by electron-beam lithography, and then the nanowires in unprotected regions were removed by SF_6 reactive ion etching. **b**, Dark-field images of the nanowires at different processing stages, showing that the combed nanowires are not perturbed by the processing. Scale bar, 5 μm. **c** and **d,** SEM images of trimmed nanowire arrays. The resist layer has been removed. Scale bars, 2 μm.

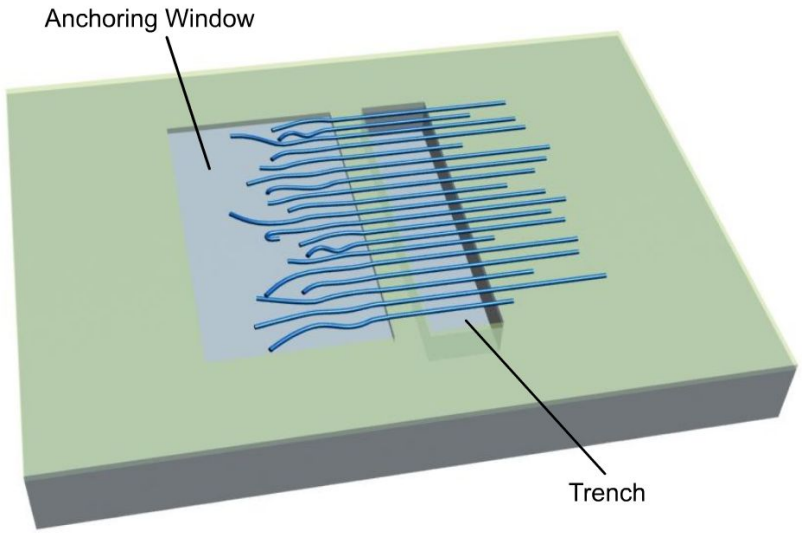

Figure S8 | Schematic of nanocombing scheme for suspended nanowire array. It corresponds to the suspended nanowire array shown in Fig. 4e in the main paper. The combing direction is left-to-right along the direction of the nanowires.

Supplementary References

1. Yan, H. *et al*. Programmable nanowire circuits for nanoprocessors. *Nature* **470**, 240-244 (2011).
2. Ferain, I., Colinge, C. A. & Colinge J.-P. Multigate transistors as the future of classical metal–oxide–semiconductor field-effect transistors, *Nature* **479**, 310-316 (2011)